# Characterization of MIMO Channels for Handheld Devices in Personal Area Networks at 5 GHz

Johan Karedal[1], Anders J Johansson[1], Fredrik Tufvesson[1], and Andreas F. Molisch[1,2]

[1] Dept. of Electroscience, Lund University, Box 118, SE-221 00 Lund, Sweden.

[2] Mitsubishi Electric Research Labs, 201 Broadway, Cambridge, MA 02139, USA.

Email: {Johan.Karedal, Anders.J.Johansson, Fredrik.Tufvesson, Andreas.Molisch}@es.lth.se

*(Invited Paper)*

*Abstract*—In this paper we analyze the properties of MIMO channels for personal area networks (PANs). Such channels differ from propagation channels in wide-area networks due to several reasons: (i) the environments in which the systems operate are different, (ii) the mobility models and ranges are different, (iii) the influence from human presence in the environment is different. In this paper, we present results from a measurement campaign for PAN channels between two handheld devices. The measurements are conducted over distances of 1-10 m using two handheld four-element antenna devices. For each distance, a number of channel realizations are obtained by moving the devices over a small area, and by rotating the persons holding the devices. We find that the correlation between the antenna elements is low. The small-scale statistics of the amplitude are well described by the Rayleigh distribution in many cases, but the effects of shadowing by the body of the operator can lead to different statistics.

## I. INTRODUCTION

In recent years there has been an increase of interest in wireless systems with high data rates but small coverage area. Such systems, commonly known as "personal area networks" (PANs), are often defined as a network where transmitter and receiver are separated no more than 10 m, and are usually within the same room. Due to the high required data rates, innovative transmission schemes have been proposed: both ultra-wideband techniques [1], [2] and MIMO (multiple-input−multiple-output) systems seem suitable. Among other investigations, the European Union has commissioned the MAGNET project that investigates different approaches to realizing PANs.

MIMO systems, i.e., systems with multiple antenna elements at both link ends, promise high spectral efficiency and thus high data rates by allowing the transmission of multiple data streams without additional spectral resources [3], [4], [5]. For this reason, many theoretical as well as experimental investigations have been performed on different aspects of MIMO in the last 10 years [6]. It has been shown repeatedly that the wireless propagation channel has a key impact on both the information-theoretical limits and the performance of practical MIMO systems [7].

However, there are, to our knowledge, only very few measurements of MIMO channels in PANs. The papers [8] and [9] treat correlation properties and capacity issues for a base-station to hand-held terminal scenario, respectively, whereas [10] focuses on the integration of antennas into a handheld device.

In the current paper, we present the results of a recent measurement campaign that deals specifically with MIMO for PANs. The measurements are performed in a modern office building at 5.2 GHz, using two handheld devices, each with several antenna elements, as transmitter and receiver, respectively. Scenarios with either Tx and Rx stationary with stationary surroundings, Tx and Rx stationary with temporally varying surroundings (moving people), or movement of the devices, are measured. Furthermore, the impact of antenna arrangements and body shadowing is taken into account.

The remainder of the paper is organized the following way: Section II covers the measurement setup, measurement environment, and data post processing. Section III describes the results concerning pathloss, delay dispersion, correlation between antenna elements, and statistics of the small-scale fading. Finally, in Section IV, a summary and conclusions is presented.

## II. MEASUREMENT SETUP

Past measurements and modeling of MIMO propagation channels concentrated mostly on scenarios that correspond to wide-area (cellular) networks [11] and wireless local area networks [12]. Those measurements have found it useful to separate the impact of the antennas from the channel, and describe the channel by its double-directional impulse response [13] or the transfer function matrix in the absence of human beings close to the "mobile station".[1] However, for PANs, especially for hand-held and body-worn devices, it is preferable to analyze the combined effect of channel, antennas, and human operators of the mobile station, using the same antenna configurations for the measurements that would also be used for the actual operation. The reasons for this are twofold: (i) the influence of the body is dominant in PANs; thus measurements of the channel transfer function matrix without humans are of limited relevance (ii) double-directional measurements cannot be easily made in PANs, because they require measurements with large antenna arrays. A double-directional channel characterization is based on the extracted parameters (delay, angle-of-arrival, angle-of-departure) of the multipath components (MPCs) and requires the use of large

---

[1]An exception is, e.g., the recent paper [14] that analyzes the impact of humans on the transfer function in wireless LANs.
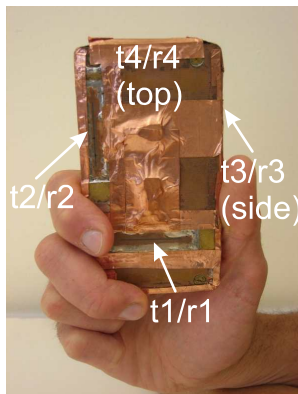
Fig. 1. One of the handheld devices, a dummy PDA clad with copper tape, with four integrated slot antenna elements marked t1/r1 (transmitter1/receiver 1), t2/r2 etc. Element 3 is on the right side of the box, whereas element four is located on the top side.
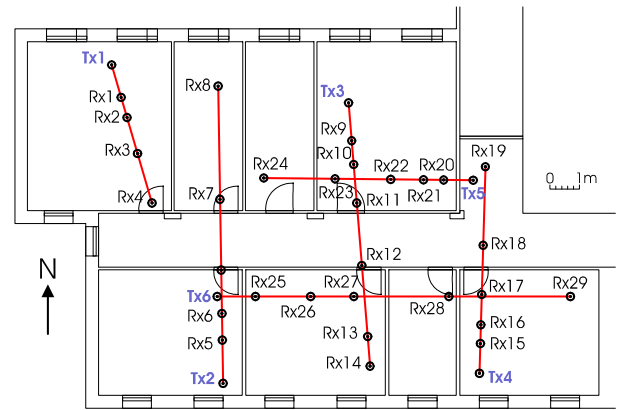


Fig. 2. Site map of the measurement positions for the static scenario. Measurements were only made between positions along the same line.
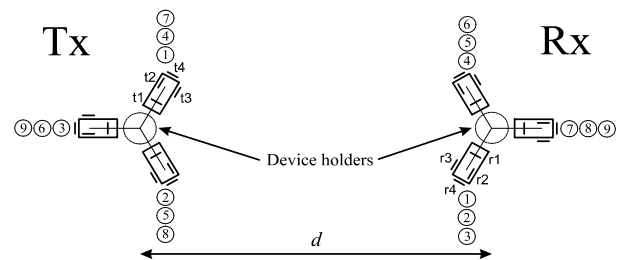


Fig. 3. The nine possible antenna orientations at each Rx position, at a distance $d$ from the Tx. The circled numbers show how Tx and Rx were oriented during each of the nine measurements, whereas t1, r1, t2, etc. show the four slot antenna elements on each handheld device.

antenna arrays that cannot be used in hand-held or body-area devices. For these reasons, our paper concentrates on the characterization of the "effective" channels that include the impact of antennas and human bodies.

The measurements were done with the RUSK LUND channel sounder that performs MIMO measurements based on the "switched array" principle [15]. The frequency band $5.2 \pm 0.1$ GHz was measured, divided into 321 frequency points. The RUSK sounder allows to adjust the length of the test signal and the corresponding guard interval between two consecutive measurements. For these measurements a value of $1.6$ $\mu$s was used for both. This corresponds to a resolvable "excess runlength" of multipath components of $480$ m, which was more than enough to avoid overlap of consecutive impulse responses.

Two identical handheld devices were used as transmitter (Tx) and receiver (Rx), respectively. Each was made of a metal box with $4$ integrated slot antenna elements. Two slots are in the front of the box, perpendicular to each other, one is on the top side, and one is in the right side of the box (see Fig. 1).

### A. The Office Environment

The measurements were performed in an office environment of the E-building at LTH, Lund University, Sweden. The building is made of reinforced concrete with gypsum wallboards separating the different offices. Throughout the offices, several different Tx and Rx positions were selected for the static measurements in order to constitute realistic antenna positions in both line-of-sight (LOS) and non-LOS (NLOS) situations. NLOS was created by placing the Tx next to a wall, then conducting measurements on the other side of that wall. Regarding LOS measurements, in this paper, we define LOS as any measurement where there is a direct optical path between the *person* holding the Tx and the *person* holding the Rx. Hence, LOS also includes cases where the person holding the antenna (henceforth called "device holders") is obstructing the path between the antennas. In total, $4$ different Tx positions were selected for LOS measurements and 2 Tx positions were

used for NLOS. For each Tx positions, a number of Rx positions were used (see Fig. 2).

Both Tx as well as Rx were held in the right hand of a standing person, and slightly tilted forward as when looking at the screen of a real PDA. At each Rx position, a number of measurements with different orientations of Tx as well as Rx (i.e., antenna plus device holder) were made. Three different rotations were used at either side, i.e., each device holder could face three different directions, $60°$, $180°$ and $300°$, with $0°$ being the direction where the device holder is facing the other device holder. With three possible directions at each side, a total of nine measurements were performed at every Rx position as illustrated in Fig. 3. These nine measurements are henceforth referred to as *orientation* $1 - 9$. Additionally, during each measurement the Tx device was slowly moved over a small area (approximately 30 cm $\times$ 30 cm) allowing the channel sounder to sample 10 slightly different snapshots of the channel with small spatial offsets. These 10 snapshots were used in the small-scale fading analysis, where they, in conjunction with the 321 frequency sub-channels, constituted the statistical ensemble. Thus, we stress that small-scale averaging does not include averaging over the 9 different orientations.

For the dynamic measurements, the measurements were performed during a time period of $5.4$ seconds, with a sample rate of $55$ measurements per second. Measurements were performed both with with moving antennas as well as with a dynamic environment (static device holders but other persons

moving around nearby). All dynamic measurements were performed just outside or in the office containing static Tx3 (see Fig. 2).

Three measurements were made with moving *antennas*. In the first, both device holders were walking slowly (0.75 m/s) towards each other in the corridor, in the second, the device holders were walking away from each other at the same speed and in the same corridor. In the third, the device holders were once again walking towards each other, but this time one device holder was walking in the corridor, while the other was walking inside the adjacent office.

The dynamic *environment* measurements were made inside this office, with Tx and Rx at each side of the room. The dynamic environment consisted of five people walking inside the room. Four different measurements were made. First, people were allowed to walk in the optical LOS path between the device holders. Two such measurements were made, one with the device holders facing each other and one where they were facing away from each other. Then, two measurements were made where the walking people were *not* allowed to step into the optical LOS path, and again one measurement was performed with the device holders facing each other, and one was performed with them facing away from each other.

## III. MEASUREMENT RESULTS

### A. Received Power

Fig. 4 shows a scatter plot of the received power (small-scale averaged over snapshots, frequency and all Tx and Rx elements) as a function of distance for the LOS scenario. We note that the distance dependent pathloss (an estimated pathloss exponent of $0.27$) in the considered range, $1 - 10$ m, has a minor influence compared to the large scale fading (note that the shadowing is created both by rotations and different measurement locations). For the NLOS scenario, the pathloss exponent is somewhat higher (estimated to $2.54$), but still the influence of the shadowing is large compared to that of the distance in the considered range.

We distinguish between three different loss components for the signal power loss: the distance-dependent path loss, small scale fading to account for small distance variations of the considered antenna elements, and large scale fading due to orientation and large position shifts of the device. The complete pathloss modeling is presented in [16].

### B. Small-Scale Fading

The amplitude statistics of the elements of the channel matrix **H** is usually of interest for a wireless channel. Hence, each of the nine orientations of every Rx position, we investigate the small-scale statistics for each combination of Tx and Rx elements, i.e., every Rx position renders a total of 16 Tx-Rx combinations $\times$ 9 orientations $=$ 144 statistical ensembles. Each statistical ensemble is, as previously mentioned (see Sec. II), made up by the 321 frequency subchannels in conjunction with the 10 spatial snapshots. Estimates of the $90\%$ and $50\%$ coherence bandwidths of the channels [17], $1.5 - 1.8$ MHz and $15 - 18$ MHz, respectively, ensures that we have enough independent samples in the frequency domain.
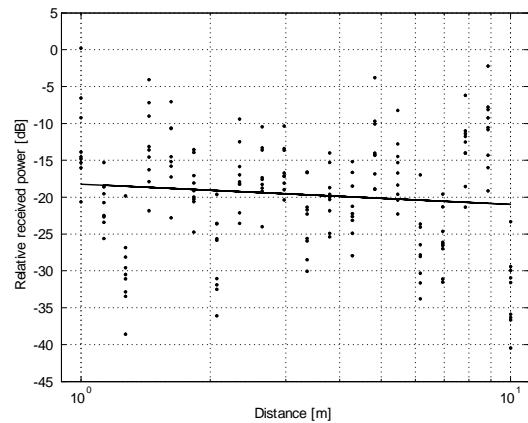


Fig. 4. Scatter plot of the received power vs. distance for all LOS measurements. For each value of the distance $d$, there are nine measurement points, corresponding to the different Tx and Rx orientations as described in Section II. The best fit regression line corresponds to a pathloss exponent $n = 0.27$.

The statistics is analyzed by fitting a Rayleigh and a Ricean distribution, with K-factors estimated using the method by Greenstein *et al.* [18]. The results show that the distribution is best described by a Ricean distribution (with a high K-factor) in some cases, and a Rayleigh distribution (or a Ricean with a low K-factor) in others, also for situations that were assumed to be LOS. It is further noted that for a single measurement, the channel between a certain two antenna elements can be Rayleigh fading, while the channel between two other elements can be Ricean, as can be seen in Fig. 5 (which is from a 9 m LOS measurement; Tx3 to Rx14, device holders in orientation 1; see Fig 3). In the figure, all channels including Rx element r4 (the element facing the *Tx* device holder) are clearly Ricean (with K-factors of 2 to 10 dB), whereas channels using Rx element r1 (the element facing the *Rx* device holder) tend to be better described by a Rayleigh distribution. Since the antenna patterns of the slot antennas are fairly directive (and with the placement of the slot antenna elements in mind; see Fig. 1), a possible explanation for this is that the antenna gain in the direction of the optical LOS for some antenna elements is very poor. Hence, the signal strength of the optical LOS path becomes weak compared to the reflected paths.

It can also be seen from Fig. 5 that some cases are not well described by neither the Rayleigh nor the Ricean distribution (see e.g., the channel between t2 and r3). To analyze this effect, we redo the statistical analysis, this time treating each snapshot as an individual measurement, i.e., the statistical ensemble is constituted of *only* the 321 frequency subchannels. The results show that there is a clear difference in the statistics of different *snapshots*, where some are well described by a Ricean distribution, whereas others are better described a Rayleigh distribution. This would be obvious for cases where either of the device holders are facing away from the other, and the small motion of the Tx device could make the optical LOS path between the antennas alternate between unobstructed in some snapshots, and obstructed by the body of
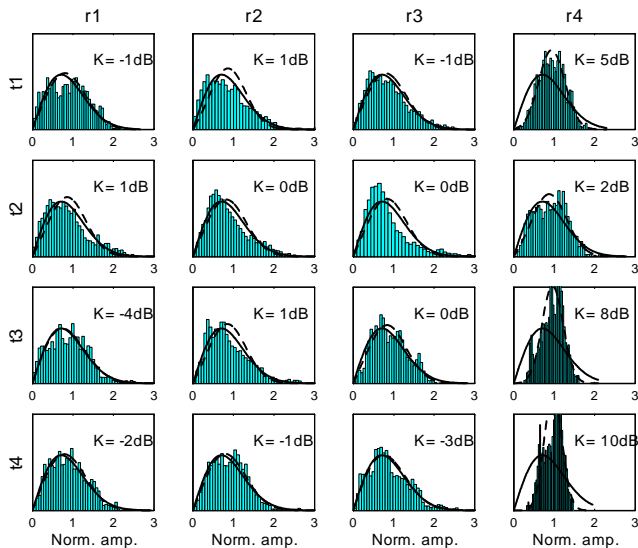
Fig. 5. Amplitude statistics for all the antenna channels of the Tx3 to Rx14 measurement, orientation 1. The figures are organized as a matrix with the Tx elements as rows and the Rx elements as columns (the indeces are written in the left and top perimeter). For each figure, a Ricean fit (dashed) and a Rayleigh fit (solid) has been made.
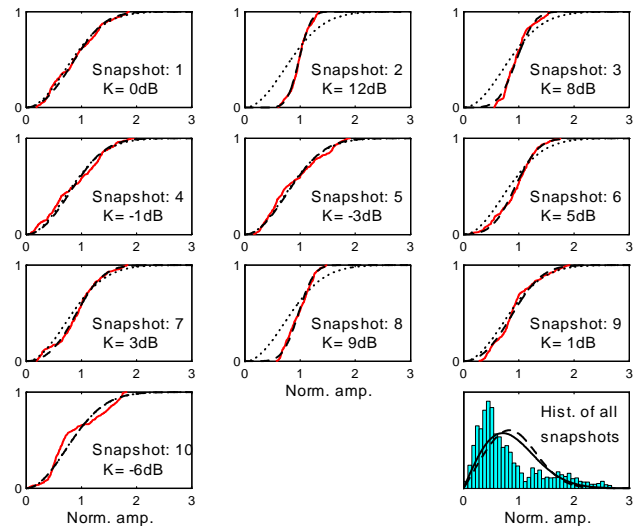


Fig. 6. Cdf:s of the amplitude statistics for each snapshot of measurement Tx3 to Rx9, rotation 1, using antenna elements t1 to r3. The solid lines are measured data, the dashed lines are best fit Riceans (with the K-factor printed in the figure), while the dotted lines are best fit Rayleighs. It is clearly seen that different snapshots have different distributions.

the device holder in others. However, this effect is also present in measurements were both human bodies are clearly out of the way (i.e., orientation 1, 2, 4 or 5). Fig. 6 shows cumulative distribution functions (cdf:s) of a 1 m LOS measurement (Tx3 to Rx9, orientation 1, Tx element t1 to Rx element r3) where snapshots 2, 3 and 8 appear Ricean distributed while the others look Rayleigh distributed. Again, an explanation for this could be the directivity of the antenna elements and the influence of the device holder's arm. Since the arm in practice becomes a part of the antenna, the radiation pattern is likely to change slightly with the small-scale movement of the device. Hence, the antenna gain in the optical LOS will change with time.

For NLOS scenarios where the Rx is close to the Tx, the amplitude statistic does not differ much from the LOS measurements. This is probably due to the gypsum wallboards separating the offices creating little attenuation. For the larger distances, however, the Rayleigh distribution is more often the better description.

### C. Antenna Correlation

A key characteristic of MIMO channels is the correlation between the entries of the channel matrix **H**. A full description of those correlations requires a correlation matrix of size $N_r N_t \times N_r N_t$, which is reasonable for the considered systems. For our measurements, we analyze the correlation for MIMO systems utilizing all elements, i.e., $4 \times 4$ systems. The mean of the magnitude of the (complex) correlation coefficient between different antennas is low, varying between $0.1$ and $0.2$, with a standard deviation around $0.1$.[2] These values are so low that zero-correlation is a sufficiently accurate model. Also, the low

[2]Due to space restrictions we cannot, however, present the full correlation matrix in the paper.

### TABLE I
MEDIAN MEAN RECEIVED POWER BETWEEN DIFFERENT ANTENNA ELEMENTS.

| [dB] | r1 | r2 | r3 | r4 |
|------|-------|-------|-------|-------|
| t1 | −19.6 | −18.5 | −19.3 | −18.7 |
| t2 | −27.3 | −25.9 | −26.4 | −26.4 |
| t3 | −20.0 | −18.6 | −18.7 | −18.8 |
| t4 | −18.1 | −16.9 | −17.5 | −17.2 |

correlation implies that a MIMO system is definitely a viable possibility.

Table I shows the median (over all Rx positions, orientations and snapshots) mean (over frequency) received powers. As can be seen from the table, the channels are almost equally strong, with the exception of channels utilizing transmit element 2.

### D. Coherence Time

To determine the coherence time of the channel we calculate the time correlation coefficients of the entries in the channel matrix for the dynamic measurements. The "aggregate walking speed" of $1.5$ m/s (see Section II) corresponds to a maximum Doppler frequency of 13 Hz. In Fig. 7 we present correlation coefficients from the 7 different measurements described in Section II. It is noted that the impact of a dynamic environment is much smaller than in the case where the antennas themselves are moving, and that the correlation coefficients exhibit a floor at values of about $0.7$. The coherence times are estimated to $T_{|\rho|=0.9} = 3.67$ ms and $T_{|\rho|=0.5} = 16$ ms for the case with moving antennas, while $T_{|\rho|=0.9} = 12.5$ ms for the case with a dynamic environment.
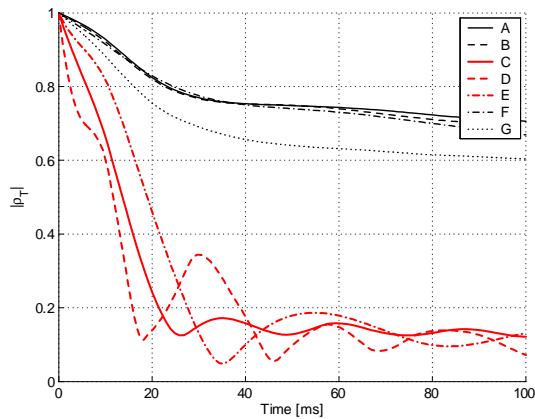
Fig. 7. Time correlation coefficient for the dynamic scenario. Lines (C, D and E) are from the measurements with moving antennas, whereas the thinner lines (A, B, F and G) belong to measurements with a dynamic environment.

## IV. SUMMARY AND CONCLUSIONS

We have presented results of an extensive measurement campaign for MIMO wireless propagation channels at $5.2$ GHz. The scenarios, antenna arrangements, and choice of locations correspond to a typical PAN using multiple antenna devices resembling PDAs. We draw the following conclusions:

- In the distance range considered for PANs, the impact of the distance dependence on the received power is minor, and shadowing effects dominate.
- The definition of LOS becomes ambiguous, as the obstruction of a direct propagation path between Tx and Rx can be due to the direction of the antenna, or the person holding the device.
- The amplitude statistics are well described by the Rayleigh distribution in many cases, whereas the Ricean distribution gives a better fit in others. This is valid for LOS as well as NLOS scenarios. A possible explanation for this lies in the directivity of the antenna patterns and the weak antenna gains sometimes associated with the optical LOS. For some measurements, the effect of body shadowing of the device holder creates amplitude statistics with a distribution given by neither the Rayleigh or the Rice distribution.
- Since the correlations between the entries of the transfer function matrix are so low, with a mean generally less than $0.2$, a zero-correlation model is sufficiently accurate for most applications.
- The coherence time of the channel (where 50% correlation is achieved) is on the order of 10 ms for the case of moving devices. For static devices with moving environment, the temporal correlation coefficient exhibits a floor of about $0.7$.

We finally conclude that these results provide further insights into the propagation mechanisms of PAN channels, and can serve as a basis for PAN system design.

## REFERENCES

[1] A. Batra et al, "Multi-band OFDM physical layer proposal," 2003. Document IEEE 802.15-03/267r2.

[2] J. McCorkle et al, "Xtreme spectrum cpf document," 2003. Document IEEE 802.15-03/154r0.

[3] G. J. Foschini and M. J. Gans, "On limits of wireless communications in a fading environment when using multiple antennas," *Wireless Personal Communications*, vol. 6, pp. 311–335, Feb. 1998.

[4] I. E. Telatar, "Capacity of multi-antenna Gaussian channels," *European Transactions on Telecommunications*, vol. 10, November-December 1999.

[5] A. Paulraj, D. Gore, and R. Nabar, *Multiple Antenna Systems*. Cambridge, U.K.: Cambridge University Press, 2003.

[6] D. Gesbert, M. Shafi, D.-S. Shiu, P. J. Smith, , and A. Naguib, "From theory to practice: An overview of MIMO space-time coded wireless systems," *IEEE J. Selected Ares Comm.*, vol. 21, pp. 281–302, 2003.

[7] A. F. Molisch and F. Tufvesson, *MIMO channel capacity and measurements*. Eurasip publishing, 2005.

[8] W. A. T. Kotterman, G. F. Pedersen, K. Olesen, and P. Eggers, "Correlation properties for radio channels from multiple base stations to two antennas on a small handheld terminal," in *Proc. IEEE Vehicular Technology Conference 2002 fall*, vol. 1, pp. 462–466, 2002.

[9] W. A. T. Kotterman, G. F. Pedersen, and K. Olesen, "Capacity of the mobile mimo channel for a small wireless handset and user influence," in *Proc. The 13th IEEE International Symposium on Personal, Indoor and Mobile Radio Communications*, vol. 4, pp. 1937–1941, 2002.

[10] C. Waldschmidt, C. Kuhnert, M. Pauli, and W. Wiesbeck, "Integration of mimo antenna arrays into hand-helds," in *Proc. Fifth IEE International Conference on 3G Mobile Communication Technologies*, pp. 16–23, 2004.

[11] 3GPP-3GPP2 Spatial Channel Model Ad-hoc Group, "Spatial channel model for MIMO systems," tech. rep., 2003. 3GPP and 3GPP2; download at http://www.3gpp.org.

[12] V. Erceg, L. Schumacher, P. Kyritsi, D. S. Baum, A. F. Molisch, and A. Y. Gorokhov, "Indoor MIMO WLAN channel models," in *Standardization drafts of IEEE 802 meeting*, (Dallas, USA).

[13] M. Steinbauer, A. F. Molisch, and E. Bonek, "The double-directional radio channel," *IEEE Antennas and Propagation Magazine*, vol. 43, pp. 51–63, Aug. 2001.

[14] J. Medbo, J.-E. Berg, and F. Harryson, "Temporal radio channel variations with stationary terminal," in *Proc. 60th IEEE Vehicular Technology Conference*.

[15] R. Thomae, D. Hampicke, A. Richter, G. Sommerkorn, A. Schneider, U. Trautwein, and W. Wirnitzer, "Identification of the time-variant directional mobile radio channels," *IEEE Trans. on Instrumentation and measurement*, vol. 49, pp. 357–364, 2000.

[16] J. Karedal, A. J. Johansson, F. Tufvesson, and A. F. Molisch, "Shadowing effects in MIMO channels for personal area networks," accepted to IEEE Vehicular Technology Conference 2006 fall.

[17] T. S. Rappaport, *Wireless Communications — Principles and Practices*. Upper Saddle River, NJ, USA: Prentice Hall, 1996.

[18] L. J. Greenstein, D. G. Michelson, and V. Erceg, "Moment-method estimation of the Ricean K-factor," *IEEE Communications Letters*, vol. 3, pp. 175–176, June 1999.